Highly Nonlinear Silicate Optical Fiber With High Intrinsic SBS Threshold

P. Dragic,[1,*] M. Tuggle,[2] C. Kucera,[2] T. Hawkins,[2] D. Sligh,[2] A.F.J. Runge,[3] A.C. Peacock,[3] and J. Ballato[2]

[1]*Department of Electrical and Computer Engineering, University of Illinois at Urbana, Champaign, Urbana, IL 61822,*
[2]*Center for Optical Materials Science and Engineering Technologies, Clemson University, Clemson, SC 29625*
[3]*Optoelectronics Research Centre, University of Southampton, Highfield, Southampton, Hampshire SO17 1BJ, UK*
[*]*Author e-mail address: p-dragic@illinois.edu*

Abstract: We report on the development of a highly nonlinear yttrium aluminosilicate optical fiber with intrinsically high SBS threshold. Large-scale SBS suppression is achieved through a combination of judicious waveguide design and material selection.

OCIS codes: (060.0060) Fiber optics and optical communications; (060.2290) Fiber materials; (060.3510) Lasers, fiber; (060.4370) Nonlinear optics, fiber [8-pt. type]; (290.5830) Scattering, Brillouin

1. Introduction

Highly nonlinear optical fibers find a wide range of applications, including Raman [1] and parametric [2] amplification, and supercontinuum generation [3]. Oftentimes systems utilizing them require a signal spectrum that leads to stimulated Brillouin scattering (SBS) being the primary power limitation. Numerous schemes have therefore been proposed to suppress it, including phase modulation [4], axial strain distributions [5], fiber segmentation (use of isolators) [6], and the use of alumina to form acoustic anti-guides [7,8]. From a practicality standpoint, the use of a single fiber with no active means to suppress SBS is most desirable, and therefore the latter method, the use of alumina, or acoustic anti-guides generally, seems particularly appealing. Alumina is known to raise the acoustic velocity when added to pure silica [9], and thus through its use the acoustic wave can be engineered to have large-scale waveguide attenuation resulting from modes that radiate away from an anti-wave-guiding core [10]. It is worthy to note that recently both MgO [11] and Li_2O [12] have been shown to possess similar properties. This may prove to be important as the availability of a wider range of materials can offer additional degrees of freedom in tailoring the dispersion characteristics of a fiber.

It also has recently been shown that the addition of several oxides to silicate glass systems affords a significant lessening of the Brillouin gain coefficient, g_B, through a substantial reduction in the net photoelasticity of the glass [13,14]. More specifically, g_B is proportional to the square of the Pockels coefficient, p_{12}. Thus the addition of some materials of negative p_{12} (such as BaO, SrO, MgO, and Al_2O_3) to silica can off-set its positive-valued constant, or even give $p_{12} = 0$ with an appropriate composition [15]. Adding to this is that these materials also bring a larger material acoustic attenuation coefficient to the glass system, decreasing the phonon lifetime through viscoelastic damping [13]. Therefore, to take advantage of both acoustic anti-wave-guidance and materials engineering, to first order, the selection rule is to identify a glass additive that has negative p_{12} and large acoustic velocity (larger than that of SiO_2). Here, for reasons relating to ease-of-fabrication, Al_2O_3 is considered.

The alumina content required to have a significant impact on p_{12} is one that is not tenable through the use of conventional fiber fabrication methods [15]. Therefore, the molten core approach has been utilized to achieve fibers possessing greater than 10 mole% Al_2O_3 [16]. Furthermore, acoustic anti-guidance is only relevant where the waveguide attenuation term is at least comparable to the material damping coefficient [10], the former being a strong function of the core diameter and its acoustic velocity relative to the silica cladding [17]. As such, to be able to control the acoustic velocity increase resulting from the addition of alumina, a velocity-reducing additive is incorporated (Y_2O_3) through the use of a multilayered molten core fabrication process. The precursor core phase consists of an inner YAG rod surrounded by a sapphire sleeve. Through careful selection of the relative sizes of these single crystal elements, the relative abundance of aluminum and yttrium sesquioxides in the melt, and therefore the acoustic velocity and refractive index, can be controlled. As is shown here with Yb, this methodology is also a means to introduce a rare earth to the aluminosilicate system. It is shown that highly nonlinear fibers can be realized with Brillouin spectra broader than those obtained by straining optical fiber [2], with one fiber exhibiting a spectrum spread across roughly 500 MHz.

2. Optical Fibers

Optical fibers were produced using the molten core method [5]. A multilayer precursor core was fabricated by inserting a rare-earth doped yttrium aluminum garnet (YAG) crystal into a commercial sapphire (Al_2O_3) sleeve. The multilayer core was then inserted into a high purity silica capillary preform tube (3mm inner and 30mm outer

diameters) to be drawn into fiber. For this study, a Yb:YAG crystal was investigated, and subsequently fiber was drawn with differing core dimensions. The preform was heated to 2000°C at which temperature the silica preform softens and the precursor materials melt and mix, as is characteristic of the molten core process. The consequential inclusion of silica results from the dissolution of the surrounding cladding material, yielding silicate compositions in the fiber core with a pure silica cladding. The preform is then drawn into a fiber, and the molten core is found kinetically trapped (i.e., quenched) into its metastable glassy state due to the high cooling rates (~2000°C/s). The drawn fibers had a glass cladding diameter of 125µm with an acrylate coating diameter of about 250µm.

TABLE I. SUMMARY OF PHYSICAL PROPERTIES OF TWO FABRICATED FIBERS

Value	Fiber 1	Fiber 2
Effective Area, A_{eff}* (μm^2, 1550 nm)	11.2	20.7
Δn (10^{-3}) at core center	47.3	32.9
g_B (10^{-11} m/W)	0.125	0.139
n_2** (10^{-20} m^2/W)	1.8	2.0
Attenuation (dB/m 1550 nm)	0.78	0.47
Dispersion* (ps/nm-km)	+9.0	-40.1
BFOM (at 1550 nm)	1.23	1.22

*Calculated from the RIP
**Estimated from SPM-based measurements

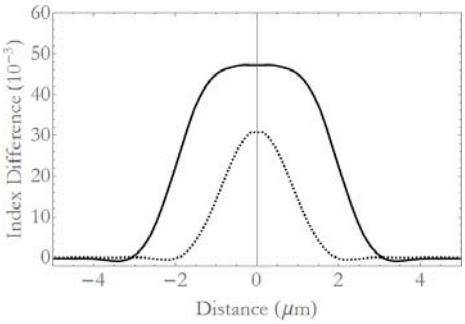

Fig.1. RIPs for Fibers 1 (solid line) and 2 (dashed line).

3. Results

Fig. 1 provides the refractive index profiles (RIPs) for the two fibers, and a summary of their characteristics may be found in Table I. The effective area and dispersion coefficients (used for measurements of n_2) are calculated from these RIPs. Also provided are the attenuation coefficients. While they are indeed still quite high for applications requiring longer fiber lengths, it is believed a large part of the loss stems from the use of industrial-grade precursors that are not optimized for purity. This is consistent with the fact that the Fiber 2 core has more high purity silica originating from the cladding and hence its attenuation is much lower.

Fig. 2 provides normalized Brillouin gain spectra for the two fibers. The strong peak near 11.0 GHz and the small one near 11.1 GHz are signatures of the measurement apparatus. These measurements were taken by collecting spontaneous Brillouin signal while pumping roughly 2 meters of fiber at 1534 nm with a narrow linewidth seed source. The Fiber 1 spectrum has a width of about 200 MHz, while that of Fiber 2 spans roughly 500 MHz. The structure in the latter spectrum could indicate the presence of higher order acoustic modes [17]. g_B was estimated for each fiber by comparing the strength of spontaneous scattering with that of a fiber of known g_B. These results are also provided in Table I. The sharp peak near the blue end of the Fiber 2 spectrum is Brillouin scattering in the cladding due to the mode being wider relative to the core; ultimately setting the SBS threshold for this fiber.

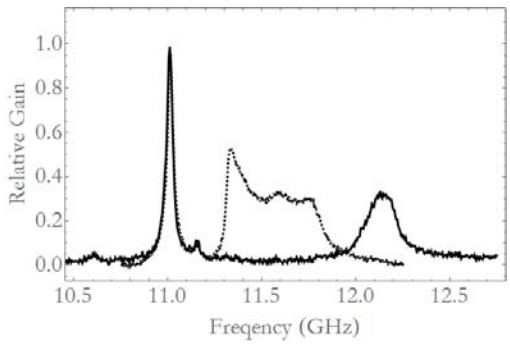

Fig. 3. Brillouin gain spectra for Fibers 1 (solid line) and 2 (dashed line). The spectra are very broad. Absolute peak values are identified in Table I.

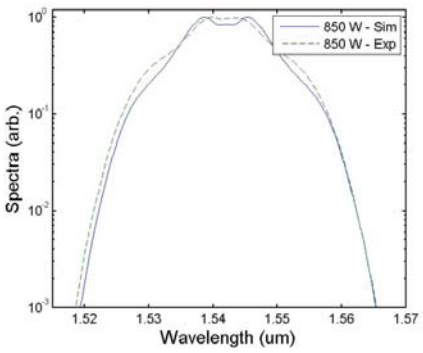

Fig. 4. Estimate of n_2 via SPM measurements. Fiber 2 data shown as an example.

The nonlinear refractive index, n_2, was estimated using self phase modulation (SPM) measurements in the two fibers. A temporally short pulse with up to 1 kW of peak power at 1542 nm was launched into one end of 5-meter

fiber segments. The output spectrum was then modeled (with a standard nonlinear Schrödinger Equation that includes the fiber attenuation) and fitted to the measured ones by adjusting the nonlinear gain coefficient. Dispersion was estimated from the RIPs and this is a primary source of uncertainty in the values for n_2. Measurements of the dispersion coefficients of the fibers are currently underway.

The estimate of n_2 now allows for the determination of the Brillouin figure of merit (BFOM) for these fibers, which is defined to be $BFOM = \gamma L_{eff} P_{th}$ [18] where γ is the nonlinear gain coefficient ($\gamma = 2\pi n_2 / \lambda A_{eff}$ with λ the optical wavelength), L_{eff} is the effective length (taking the attenuation into consideration), and P_{th} is the SBS threshold power. If P_{th} is simply defined as in [19], then $L_{eff} P_{th} = 21 A_{eff} / g_B$ and a simplified form is obtained: $BFOM = 42\pi n_2 / \lambda g_B$. The pre-factor value of 21 is known to vary depending on the shape and width of the Brillouin gain spectrum, but offers a reasonable approximation in the present case. The BFOM for each fiber can be found in Table I. Due to very low intrinsic Brillouin gain coefficients, both fibers have similar BFOM values that are comparable to those realized for both Ge- and Al-doped fibers with 1 kg of axially-gradient applied strain [18]. SBS is cladding-limited in Fiber 2, but it is believed that further reductions in g_B are possible. Other data will be discussed at the conference, including the measured Sellmeier coefficients of the individual glass constituents. Other potential glass additives, such as MgO, will also be briefly described. Paths to improving the present results will be outlined.

4. References

[1] G. Mélin, D. Labat, L. Galkovsky, A. Fleureau, S. Lempereur, A. Mussot, and A. Kudlinski, "Highly-nonlinear photonic crystal fiber with high figure of merit around 1 μm," Electron. Lett. **48**, 232-234 (2012).

[2] C. Lundström, R. Malik, L. Grüner-Nielsen, B. Corcoran, S.L.I. Olsson, M. Karlsson, and P.A. Andrekson, "Fiber Optic Parametric Amplifier With 10-dB Net Gain Without Pump Dithering," IEEE Photon. Technol. Lett. **25**, 234-237 (2013).

[3] S.-S. Lin, S.-K. Hwang, and J.-M. Liu, "Supercontinuum generation in highly nonlinear fibers using amplified noise-like optical pulses," Opt. Express **22**, 4152-4160 (2014).

[4] S. K. Korotky, P. B. Hansen, L. Eskildsen, and J. J. Veselka, "Efficient phase modulation scheme for suppressing stimulated Brillouin scattering," in Proc. Technol. Dig. Conf. Integr. Opt. Fiber Commun., 1995, pp. 110–111.

[5] J. M. C. Boggio, J. D. Marconi, and H.L. Fragnito, "Experimental and numerical investigation of the SBS-threshold increase in an optical fiber by applying strain distributions," J. Lightwave Technol. **23**, 3808–3814 (2005).

[6] Y. Takushima and T. Okoshi, "Suppression of simulated Brillouin scattering using optical isolators," Electron. Lett. **28**, 1155–1157 (1992).

[7] T. Nakanishi, M. Tanaka, T. Hasegawa, M. Hirano, T. Okuno, and M. Onishi, "AlO-SiO core highly nonlinear dispersion-shifted fiber with Brillouin gain suppression improved by 6.1 dB," in Proc. ECOC 2006, Cannes, France, vol. 6, pp. 17–18, Paper TH.4.2.2.

[8] P.D. Dragic, C.-H. Liu, G.C. Papen, and A. Galvanauskas, "Optical Fiber with an Acoustic Guiding Layer for Stimulated Brillouin Scattering Suppression," CLEO Technical Digest, paper CThZ3 (2005).

[9] C.K. Jen, "Similarities and differences between fiber acoustics and fiber optics," Proc. IEEE Ultrasonics Symp., 1128–33 (1985).

[10] P.D. Dragic, "Brillouin suppression by fiber design," presented at the IEEE Photonics Society Summer Topicals Meeting, paper TuC3.2, 19-21 July 2010.

[11] A. Mangognia, C. Kucera, J. Guerrier, J. Furtick, T. Hawkins, P.D. Dragic, and J. Ballato, "Spinel-derived single mode optical fiber," Opt. Mater. Express **3**, 511-518 (2013).

[12] P.D. Dragic, C. Ryan, C.J. Kucera, M. Cavillon, M. Tuggle, M. Jones, T.W. Hawkins, A.D. Yablon, R. Stolen, and J. Ballato, "Single- and few-moded lithium aluminosilicate optical fiber for athermal Brillouiin strain sensing," Opt. Lett. **40**, 5030-5033 (2015).

[13] J. Ballato and P. Dragic, "Rethinking Optical Fiber: New Demands, Old Glasses," J. Am. Ceram. Soc. **96**, 2675-2692 (2013).

[14] M. Cavillon, J. Furtick, C.J. Kucera, C. Ryan, M. Tuggle, M. Jones, T.W. Hawkins, P. Dragic, and J. Ballato, "Brillouin Properties of a Novel Srontium Aluminosilicate Glass Optical Fiber," J. Lightwave Technol. **34**, 1435-1441 (2016).

[15] P. Dragic, T. Hawkins, P. Foy, S. Morris, and J. Ballato, "Sapphire-derived all-glass optical fibers," Nat. Photon. **6**, 627-633 (2012).

[16] S.Morris and J. Ballato, "Molten Core Fabrication of Novel Optical Fibers," Am. Ceram. Soc. Bull. **92**, 24-29 (2013).

[17] P.D. Dragic, P.-C. Law, and Y.-S. Liu, "Higher order modes in acoustically antiguiding optical fiber," Microw. Opt. Technol. Lett. **54**, 2347-2349 (2012).

[18] L. Grüner-Nielsen, S. Herstrom, S. Dasgupta, D. Richardson, D. Jakobsen, C. Lundström, P.A. Andrekson, M.E.V. Pederson, and B. Pálsdóttir, "Silica-Based Highly Nonlinear Fibers with a High SBS Threshold," IEEE Winter Topicals (WTM) 2011, paper MD3.2.

[19] R.G. Smith, "Optical Power Handling Capacity of Low Loss Optical Fibers as Determined by Stimulated Raman and Brillouin Scattering," Appl. Opt. **11**, 2489-2494 (1972)**.**